BNL-224844-2023-COPA

Status of Neutronic Model Improvements for the NBSR LEU Conversion - BNL Support

C. Lu

Submitted to the 2023 ANS Winter Conference and Expo Conference
to be held at Washington, D.C.
November 12 - 15, 2023

Nuclear Science and Technology Department
Brookhaven National Laboratory

U.S. Department of Energy
USDOE Office of Science (SC), Nuclear Physics (NP) (SC-26)

DISCLAIMER

Status of Neutronic Model Improvements for the NBSR LEU Conversion – BNL Support

Cihang Lu, Peter Kohut, Athi Varuttamaseni, Lap-Yan Cheng, and Arantxa Cuadra

Brookhaven National Laboratory, Nuclear Science and Technology Department, Upton, New York, USA
clu@bnl.gov, kohut@bnl.gov, avarutta@bnl.gov, cheng@bnl.gov, acuadra@bnl.gov

INTRODUCTION

The National Bureau of Standards Reactor (NBSR) is a heavy-water (D_2O)-moderated-and-cooled tank-type reactor operating at the National Institute of Standards and Technology (NIST) with a nominal thermal power level of 20 MW [1]. The NBSR is currently fueled with U_3O_8 in an aluminum powder dispersion, cladded in aluminum alloy. With a ^{235}U enrichment of 93 ± 1 wt.%, the fuel is classified as High Enriched Uranium (HEU) [2]. Under the Global Threat Reduction Initiative (GTRI, now known as the Materials Management and Minimization program), efforts are being made to convert U.S. research reactors and isotope production facilities from the use of HEU to Low Enriched Uranium (LEU), including the NBSR. The fuel core for the LEU conversion of the NBSR is U-10Mo (uranium with 10 wt.% molybdenum) metal alloy foils with aluminum alloy cladding, the ^{235}U enrichment of which is 19.75 ± 0.2 wt.%. Only the fuel composition, fuel core thickness and volume, and aluminum cladding thickness will be changed during the conversion, whereas the overall geometry of the fuel plates and the fuel elements will remain unchanged [3]. Table 1 compares of HEU and LEU fresh fuel parameters.

Table 1. HEU and LEU fresh fuel parameters.

Parameter	HEU	LEU
^{235}U mass (g/element)	350	383
^{238}U mass (g/element)	26	1556
O mass (g/element)	68	0
Al mass (g/element)	625	0
Mo mass (g/element)	0	215
Total mass (g/element)	1069	2154
Fuel density (g/cm^3)	3.61	17.2
Fuel core thickness (cm)	0.0508	0.0215
Fuel volume (cm^3/element)	296	125.28

Studies for the NBSR LEU conversion have been conducted at Brookhaven National Laboratory (BNL), which submitted the Preliminary Safety Analysis Report (PSAR) in 2014 to the U.S. Nuclear Regulatory Commission (NRC) for review prior to conversion [3]. The neutronics calculations were performed with the Monte Carlo neutronics code MCNP 6.2 [4], and the depletion calculations were performed with the default MCNP depletion solver. This paper summarizes the improvements made to the MCNP model, previously used for the conversion PSAR, to support the conversion of the NBSR to LEU.

THE NBSR

The NBSR core consists of 30 fuel elements arranged in a hexagonal array. Among the 30 NBSR fuel elements, 16 stay in the core for eight 38.5-day cycles, whereas 14 remain in the core for seven 38.5-day cycles. With an overall length of 1.75 m, each NBSR fuel element contains an upper and a lower fuel section separated by a 17.78 cm gap. This "split-core" design maximizes the thermal neutron flux in the center of the gap for neutron scattering experiments [1]. The NBSR employs the Material Testing Reactor (MTR) plate-type fuel elements [5]. Seventeen (17) fuel plates are placed between two unfueled end plates in each fuel section, bounded by two side plates, as illustrated in Fig 1. The NBSR reactivity is controlled with four semaphore-type shim safety arms and a single automatic regulating rod.

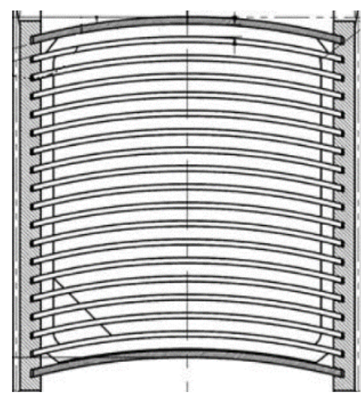

Fig 1. Cross-sectional view of a typical NBSR fuel element [3].

INCREASED FUEL MATERIAL NUMBER

The MCNP NBSR model employed for the PSAR consisted of 60 distinguished fuel materials, assuming uniform fuel material compositions in each of the upper and lower fuel elements (30×2=60). The different fuel materials in multiple plates of each fuel element, and in different axial levels and transverse stripes of each fuel plate were not considered. Using this relatively small number of fuel materials led to overpredicted peak power density because depletion calculations performed over an entire half-element with one uniform fuel material neglected the self-shielding effects near the axial mid-plane, where the thermal neutron flux peaked.

In order to provide a better prediction of maximum fission density, which is a parameter that influences the LEU fuel qualification, 900 distinguished fuel materials are now considered (30×2×3×5=900) instead of 60. Further increasing the number of materials should improve the fidelity of the neutronics calculations, but it also demands more computational power. In the improved model, there are 5 axial material zones per half-element, and 3 material zones for the 17 fuel plates, representing the two outside plates (plates 1 and 17), the next two inner plates (plates 2 and 16), and the rest of fuel plates (plates 3 - 15). The power/fission density was tallied with 14×3 meshes in 2cm×2cm cells for each plate in each half-element, as shown in Fig 2. Sensitivity studies have been performed and the mesh size of 2cm×2cm was proved adequate.

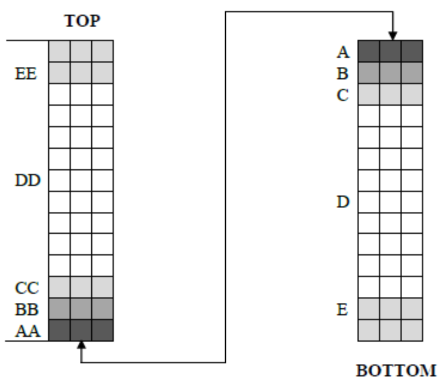

Fig 2. Axial fuel material zones and power meshes in a fuel plate.

IMPACT ON REACTIVITY

Table 2 compares the shutdown reactivity, shutdown margin, and excess reactivity predicted by the NBSR MCNP models for the startup phase (SU) at the equilibrium state with two different numbers of fuel materials. The excess reactivity was calculated with all control elements (including the four semaphore-type shim safety arms and the single automatic regulating rod) fully withdrawn. The shutdown reactivity was calculated with all control elements fully inserted. The shutdown margin was calculated considering that three of the four shim arms were fully inserted and the other one was fully withdrawn.

Table 2. Comparisons of reactivity, shutdown margin, and excess reactivity (%Δk/k) at the equilibrium state.

Number of fuel materials	60	900
Shutdown reactivity	-18.3	-17.9
Shutdown margin (shim 1 out)	-12.2	-11.9
Shutdown margin (shim 2 out)	-11.2	-10.9
Shutdown margin (shim 3 out)	-10.8	-10.3
Shutdown margin (shim 4 out)	-11.9	-11.6
Excess reactivity (all shim out)	6.30	6.48

The slightly different results were caused by the different numbers of fuel materials tracked as well as the updated nuclear data library (including fission yields and decay data) from ENDF/B-VII.0 to ENDF/B-VII.1.

IMPACT ON POWER DISTRIBUTION

Fig 3 compares the radial power distributions for the SU at the equilibrium state, as predicted by the NBSR MCNP models with different numbers of fuel materials. Higher relative powers are colored brown and lower relative powers are colored green. The half-element relative power was calculated as the half-element power divided by 333.33 kW (20 MW ÷ 60 half-element = 333.33 kW/half-element). The maximum relative difference in relative power (1.5%) was smaller than the standard deviation of the power density (assumed as 4%) used to determine thermal limits [3].

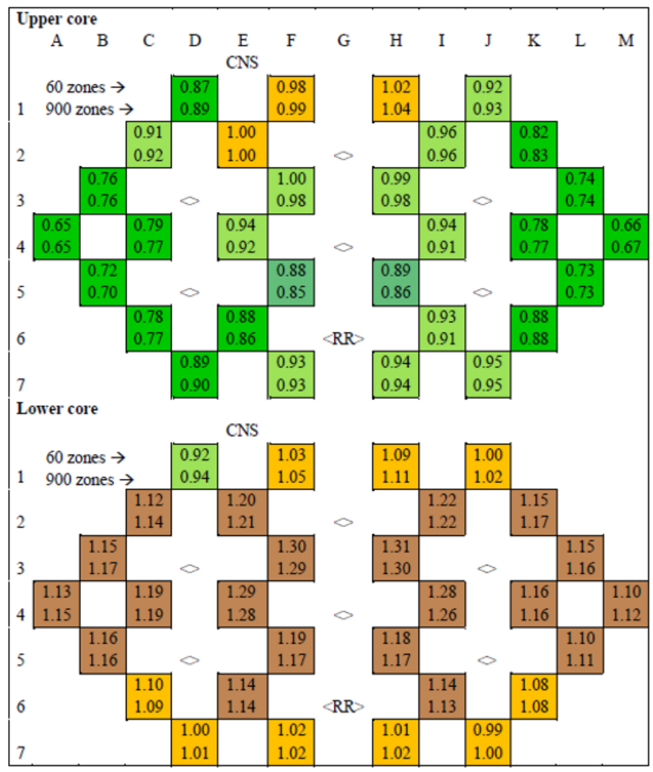

Fig 3. Half-element relative power at the startup phase.

Fig 4 compares the axial power distribution averaged over a fresh fuel element as a function of axial mesh, calculated with the MCNP NBSR models with different numbers of fuel materials. In addition to those calculated with 60 and 900 fuel materials, the results obtained with 360 fuel materials [7] are also included as an intermediate step. Similar results were observed because all the models had the same fuel composition in every axial location in every plate in the fresh fuel elements. However, power distributions calculated with different models deviated with increasing fuel depletion due to the different numbers of fuel materials considered. Fig 5 shows the average axial power distributions in a 5th-cycle fuel element. Compared to that in the 60-fuel-material model, the power near the midplane gap was lower in the 360- and 900-fuel-material models because of the localized burnup of ^{235}U in the meshes adjacent to the midplane (due to the higher thermal neutron flux). The differences in axial power became more pronounced with an increasing fuel burnup, as shown in Fig 6 for an 8th-cycle fuel element.

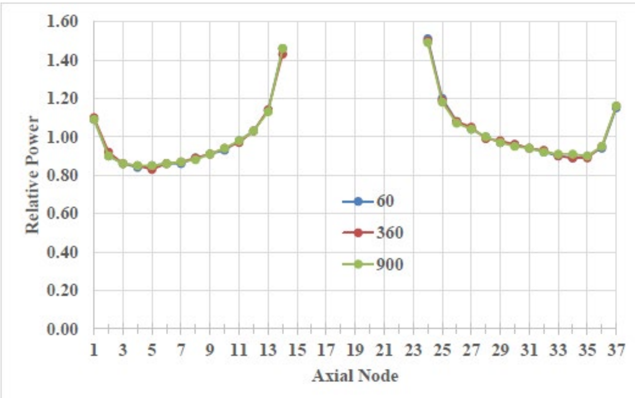

Fig 4. Axial relative power in a fresh fuel element.

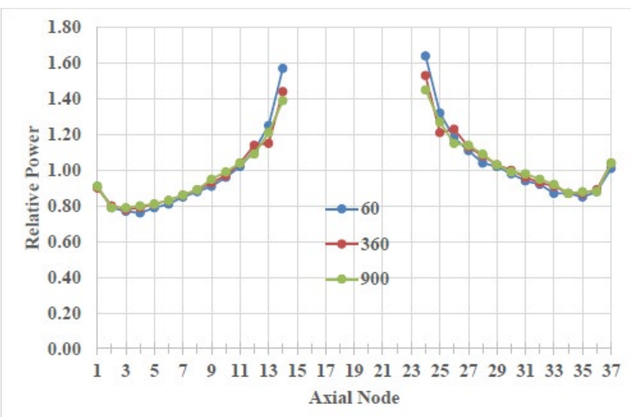

Fig 5. Axial relative power in a 5th-cycle fuel element .

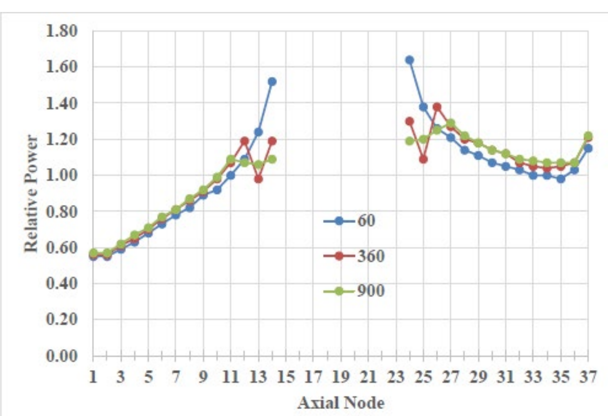

Fig 6. Axial relative power in an 8th-cycle fuel element .

IMPACT ON FISSION DENSITY

The fission density F^i accumulated in one fuel cycle (i) was calculated from the equation below:

$$F^i = \frac{\kappa}{V}\sum_n P_n \Delta t_n$$

where

- P_n is the fuel cell power (MW),
- Δt_n is the depletion interval of depletion step n,
- κ is the conversion factor, 2.679×10^{21} fissions/MWday, calculated from

$$1\ MWday = 1\ MWday \times 86400\frac{s}{day} \times\ 6.242 \times 10^{18}\frac{MeV}{MJ} \div 201.3\frac{MeV}{fission} = 2.679 \times 10^{21}\ fissions$$

- V is the volume of a fuel cell.

The three depletion steps used (n=1 to 3) were 1.5 days from SU to the Beginning of Cycle state (BOC), 17.5 days from BOC to the Mid of Cycle state (MOC), and 19.5 days from MOC to the End of Cycle state (EOC). The fission density in a fuel cell accumulates over seven or eight cycles. Fig 7 compares the fission density (in the fuel cell with the highest fission density) of the models with different numbers of fuel materials through the eight cycles. By increasing the number of fuel materials from 60 to 900, the predicted maximum fission density decreased by 22%, from 8×10^{21} fissions/cm^3 to 6.2×10^{21} fissions/ cm^3.

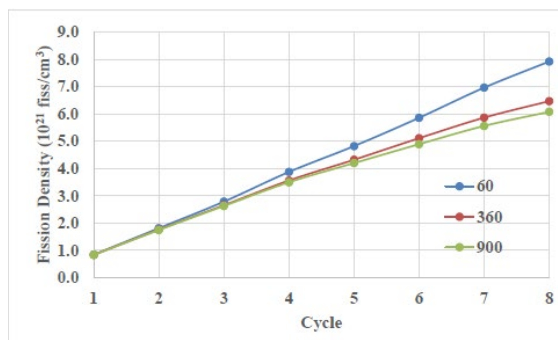

Fig 7. Comparison of the accumulated fission densities.

MODELING THE CURVED FUEL PLATES

MCNP models with curved fuel plates to better reflect reality (instead of approximating with flat fuel plate) are being considered. The fuel plates have been historically modeled as flat for simplification, as shown in Fig 8, the impact of which is currently being studied [8]. A single-assembly curved-fuel-plate model was constructed strictly according to the NBSR design drawings [9], as shown in Fig 9. It was found that the curved-fuel-plate model (k_{eff} = 1.22465 ± 0.00019) predicted a k_{eff} ~ 300 pcm lower than the flat-fuel-plate model (k_{eff}= 1.22773 ± 0.00019). Modeling the whole NBSR core with curved fuel plates, as shown in Fig 10, is being pursued.

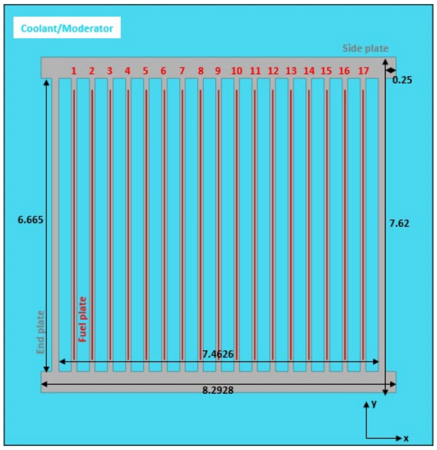

Fig 8. Cross-sectional view of the single-element flat-fuel-plate model.

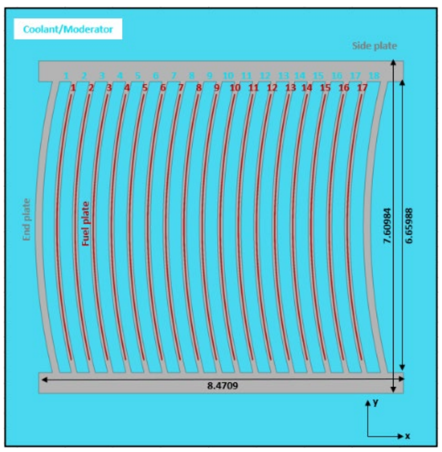

Fig 9. Cross-sectional view of the single-element curved-fuel-plate model.

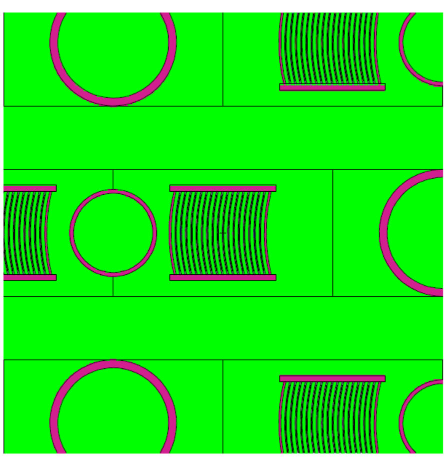

Fig 10. A zoomed view of the NBSR whole-core model with curved fuel plates.

OTHER IMPROVEMENTS IMPLEMENTED

In addition to the increased number of fuel materials considered and the more precise fuel plate geometry, several other improvements have been (or are being) made to the MCNP NBSR model. For example, temperatures have been specified for fuel (350K), coolant (318.7K), and the cold neutron source (20K). Python scripts were written to automate the fuel shuffling for the MCNP calculations [10]. Fast neutron fluence has been calculated to support the structural analysis. In addition, the impact of the aluminum alloy compositions and the fuel compositions are being analyzed to support the fuel fabrication specification impact studies.

REFERENCES

1. NIST staff, “Safety Analysis Report (SAR) for License Renewal for the National Institute of Standards and Technology Reactor - NBSR; NBSR 14, Rev 4,” National Institute of Standards and Technology. 2010.
2. R. G. Muranaka, “Conversion of Research Reactors to Low-Enrichment Uranium Fuels,” IAEA Bull 25(1), pp. 18–20. 1983.
3. D. J. Diamond, J. S. Baek, A. L. Hanson, L.-Y. Cheng, N. R. Brown, A. Cuadra, “Conversion Preliminary Safety Analysis Report for the NIST Research Reactor,” BNL-107265- 2015-IR, Brookhaven National Laboratory, December 30, 2014.
4. C. J. Werner (editor), "MCNP Users Manual - Code Version 6.2", Los Alamos National Laboratory, report LA-UR-17-29981 (2017).
5. D. W. Nigg and K. A. Steuhm, “Advanced Test Reactor Core Modeling Update Project Annual Report for Fiscal Year 2012,” Idaho National Laboratory. INL/EXT-12-27059. 2012.
6. J. S. Baek, A. L. Hanson, L. Y. Cheng, and N. R. Brown, “Analysis of Loss-of-flow Accidents for the NIST Research Reactor with Fuel Conversion from HEU to LEU,” Nuclear Technology 189, pp. 71-86. 2015.
7. P. Kohut and D. Diamond, “Increasing Compositions in NBSR Neutronics Model,” BNL- 210826-2018-INRE, Brookhaven National Laboratory, December 28, 2018.
8. C. Lu, A. Cuadra, P. Kohut, and L.-Y. Cheng, Neutronic simulation of curved fuel plate with flat plate geometry. RERTR 2022 - 42nd international meeting. October 3-5, 2022. Vienna, Austria.
9. NIST, “NIST flat short fuel plate, Rev. 3”, Drawing No. 04-100-08, 2020.
10. C. Lu and P. Kohut, “The NBSR MCNP model fuel shuffling program,” Technical report. BNL-USHPRR22-02.0, 2022.